THE NESDIS/CIMSS WINDS ALGORITHM: CURRENT STATUS AND FUTURE IMPROVEMENTS

W. Paul Menzel[1] and Robert T. Merrill[2]

[1]NESDIS and [2]CIMSS
1225 West Dayton Street
Madison, WI 53706

ABSTRACT

In support of its mission to further the application of satellite based measurements to meteorology, the Cooperative Institute for Meteorological Satellite Studies (CIMSS) has been continually developing a winds algorithm since 1987. Improvements in winds processing are tested and made available for operational winds production by the NESDIS Synoptic Analysis Branch. Recent examples are improved height assignments using the CO_2 slicing technique and automated editing based on a recursive filter with data quality weights. This paper presents some early results of the NESDIS/CIMSS wind algorithm and discusses possible modifications to the CO_2 height assignment in order to account for multiple cloud layers.

1. Introduction

Cloud motions apparent in a sequence of geostationary satellite images represent an important source of meteorological information, especially over the oceans. However, improvements in data assimilation and numerical weather prediction (NWP) have outpaced improvements in satellite derived cloud motion vector (CMV) production over the past decade, and the reduced impact of CMVs has caused the National Meteorological Center (NMC) to restrict and the European Centre for Medium range Weather Forecast (ECMWF) to discontinue the use of upper level vectors. The primary reason cited is a large slow bias, especially in and near jet cores.

Currently the main problem of CMV production is assigning cloud tracked motions to the correct heights. Thin clouds which are most likely to be passive tracers of the flow at a single level are the best tracers, but unfortunately their height assignments are especially difficult. Since the emissivity of the cloud is less than unity by an unknown and variable amount, its brightness temperature (T_b) in the infrared window is an overestimate of its actual temperature. Thus heights for thin clouds inferred directly from the observed T_b and an available temperature profile are systematically low .

Height assignment errors carry a heavy penalty because of vertical wind shear, which is greatest near regions of active weather. For this

reason, recent winds research at the Cooperative Institute for Meteorological Satellite Studies (CIMSS) has emphasized improved height assignments. A two-channel method using the "CO2 slicing" approach (Menzel et al. 1983) has been developed at CIMSS and incorporated into the CIMSS experimental winds algorithm (Merrill 1989).

Following encouraging tests in 1990, the CIMSS experimental winds algorithm was installed as a prototype operational package for NESDIS in 1991. This paper describes the upgraded winds algorithm, discusses the scientific basis of the height assignment, and presents some preliminary results.

2. The NESDIS/CIMSS automated wind algorithm

The Synoptic Analysis Branch (SAB) of the Satellite Services Division of NESDIS produces western hemisphere CMV coverage in support of NMC global numerical weather prediction and enhanced regional coverage in support of the National Hurricane Center (NHC). Low-level winds are produced using an automated "picture-pair" correlation algorithm (Green et al., 1975). These winds are produced for the full disk from infrared window channel imagery on the NMC computer system. Middle- and upper-level winds, formerly produced interactively, will be produced with the automated windco procedure in the new NESDIS/CIMSS wind algorithm on the VAS Data Utilization Center (VDUC) computer.

A flow chart of the automated winds algorithm is shown in Figure 1 and its operation is summarized below. A detailed description may be found in the literature (Merrill et al., 1991; Merrill, 1989). The procedure is applied to three successive infrared window images at thirty minute intervals.

A target selector divides the entire image into a number of cells (roughly 100 km on a side), and within each cell attempts to select a point associated with a maximum in brightness and gradient, subject to some conditions on the overall brightness and contrast of the scene. The height of the cloud feature is also computed at this stage (see the following section).

The tracking algorithm is then applied for each target point. A tracking area (24 by 24 pixels) is centered on the target in the first image. The algorithm then goes to the second image in the loop and searches for the area which best matches the radiances in the tracking area. To minimize computational expense, the search is confined to a "search area" (38 by 38 pixels) centered around the guess displacement of the target, determined from the forecast wind field interpolated to the assigned height of the tracer. The pattern matching algorithm is identical to that used for NESDIS manual winds. If a successful match is found, the indicated displacement is used to position a new tracking area on the second image and a new search area on the third, and the process is repeated. The two vectors are then averaged to produce a final wind estimate.

Three forms of quality control are then applied. First, the pair of vectors produced from the three images are compared, and if they differ by 5 m/s or more in either component, the report is flagged and not used. Instances when the system is tracking a coastline or topographic feature are also flagged. Second, an objective autoeditor is applied which edits and/or adjusts the assigned CMV height; a recursive filter with data quality weights is used to optimize the CMV based on comparison with neighboring vectors and the first guess (see paper by Hayden in this proceedings). Sometimes as many as half of the initial winds are adjusted at this stage; roughly ten percent of the initial winds are deleted. Third, the remaining winds are then displayed on the VDUC and edited manually by checking for consistency and by comparing with the first guess and rawinsondes (if available).

3. Improved height assignment

The most important upgrade to the NESDIS winds capability is improved cloud motion vector height assignment. Estimates of the pressure of a given cloud element are made with a combination of the CO_2 slicing technique and the infrared window histogram technique.

The CO_2 slicing technique is founded in the calculation of radiative transfer in an atmosphere with a single cloud layer. For a given cloud element the radiance observed, $R(\nu)$, in spectral band ν can be written

$$R(\nu) = (1 - N\epsilon)\, R_{cl}(\nu) + N\epsilon * R_{bcd}(\nu) \qquad (1)$$

where $R_{cl}(\nu)$ is the corresponding clear sky radiance, $R_{bcd}(\nu)$ is the corresponding radiance if the field of view were completely covered with an opaque cloud, N is the fraction of the field of view covered with cloud, and ϵ is the cloud emissivity. This can be transformed into

$$R(\nu) = R_{cl}(\nu) - N\epsilon \int_{P_c}^{P_s} \tau(\nu,p) \frac{dB[\nu,\, T(p)]}{dp}\, dp \qquad (2)$$

where P_s the surface pressure, P_c the cloud pressure, $\tau(\nu,p)$ the fractional transmittance of radiation of frequency ν emitted from the atmospheric pressure level (p) arriving at the top of the atmosphere (p = 0), and $B[\nu,T(p)]$ is the Planck radiance of frequency ν for temperature T(p). The second term on the right represents the decrease in radiation from clear conditions introduced by the cloud. For a given observed radiance, if the emissivity is overestimated then the cloud top pressure is also (putting it too low in the atmosphere).

To assign a cloud top pressure to a given cloud element, the ratio of the deviations in observed radiances (which include clouds) from the corresponding clear air radiances for the infrared window in the CO_2 channels is calculated from observations with VAS and from radiative transfer calculations.

$$\frac{R(\nu_1) - R_{cl}(\nu_1)}{R(\nu_2) - R_{cl}(\nu_2)} = \frac{\epsilon_1 \int_{P_s}^{P_c} \tau(\nu_1,p) \frac{dB[\nu_1, T(p)]}{dp} dp}{\epsilon_2 \int_{P_s}^{P_c} \tau(\nu_2,p) \frac{dB[\nu_2, T(p)]}{dp} dp} . \quad (3)$$

Assuming the emissivities of the two channels are roughly the same, then one has an expression by which the cloud top pressure of the cloud within the FOV can be specified. The left hand side of the equation is evaluated using observed radiances for the two channels and clear radiances computed from the first guess sounding and analyzed surface temperatures interpolated to the target point. The right hand side is then computed for a series of possible cloud pressures, and the tracer is assigned that pressure which satisfies the equation.

For the cloud motion vector height assignment, the CO_2 ratio technique is applied to the 13.3 micron channel (VAS band 5) and the longwave infrared window channel (VAS band 8). These channels have been suggested in the work of Eyre and Menzel (1989) because the 13.3 micron channel is sensitive to radiation emitted from most tropospheric features, yet the transmittance through the atmosphere is different enough from the 11 micron channel to produce a noticeable contrast. Additionally, the emissivity of thin cirrus clouds in these two spectral bands has been found to be very similar.

The observed radiances used in the above calculation are obtained using a "cold sampling" procedure. Data are taken from an area roughly 100 km on a side, centered on the target point, and a histogram of the infrared window brightness temperatures is calculated. Radiances for both channels are averaged for the coldest 25% of the pixels in the window channel. The histogram is also used to modify the surface (skin) temperature that appears in the computation of the clear column radiance; the warmer of the 90th percentile T_b and the analyzed surface temperature (using model forecast and surface reports) is used in the forward calculation.

The CO_2 ratio height fails when the difference between the observed and clear radiances in either channel is less than the instrument noise (.2 mW/m2/ster/cm-1 for 11.1 micron and 1.5 mW/m2/ster/cm-1 for 13.3 micron). This happens for low broken cloud or very thin cirrus. Another difficulty occurs for very high opaque cloud, where the clear-cloudy differences between the channels are nearly identical and the ratio is almost invariant with pressure above a certain altitude. In this situation the window channel estimate is adequate.

A window channel estimate of the cloud height is made by averaging the infrared window T_bs of the coldest 25 percent of pixels and interpolating to a pressure from the guess sounding. In an attempt to minimize the underestimate of cloud height caused by transmissive

clouds, the infrared window histogram technique considers only the coldest 1 or 2% of the histogram of T_bs within the target area and takes this average to be the cloud temperature which is used to infer cloud height (Merrill, 1989). The final height is selected from the window channel estimate, the histogram estimate, and the CO_2 slicing estimate. Estimates of 149 mb or higher are eliminated, and the highest of those which remain is selected. Periodic inspection is revealing that about 70 percent of the cloud motion heights are assigned by the CO_2 slicing method and the remainder are assigned by the infrared window histogram method.

4. Errors associated with the presence of a lower cloud layer

The CO_2 slicing algorithm assumes that there is only one cloud layer. However, for over 50% of satellite reports of upper tropospheric opaque cloud, the ground observer indicates additional cloud layers below (Menzel et al., 1991). To understand the effects of lower cloud layers, consider the radiation sensed in a cloudy field of view. For a semi-transparent or cirrus cloud layer, the radiation reaching the satellite, R_{cld}, is given by

$$R_{cld} = R_a + \epsilon * R_c + (1-\epsilon) * R_b \qquad (4)$$

where R_a is the radiation coming from above the cloud, R_c is the radiation coming from the cloud itself, R_b is the radiation coming from below the cloud, and ϵ is the cloud emissivity. When a lower cloud layer is present under the semi-transparent or cirrus cloud, R_b is smaller (i.e., some of the warmer surface is obscured by the colder cloud). If prime indicates a two layer cloud situation of high semi-transparent cloud over lower cloud, and no prime indicates the single layer high semi-transparent cloud, then

$$R_b' < R_b, \qquad (5)$$

which implies

$$R_{cld}' < R_{cld}. \qquad (6)$$

Thus the difference of cloud and clear radiance is greater for the two layer situation,

$$[R_{clr} - R_{cld}'] > [R_{clr} - R_{cld}] . \qquad (7)$$

The effect of two cloud layers is greater for the 11.0 micron channel than for the 13.3 micron channel, because the 11.0 micron channel "sees" lower into the atmosphere. So

$$[R_{clr}(11.0) - R_{cld}'(11.0)] > [R_{clr}(13.3) - R_{cld}'(13.3)]. \qquad (8)$$

This reduces the ratio of the clear minus cloud radiance deviation in Eq. (3) because the denominator is affected more than the numerator (when the less transmissive channel is in the numerator),

$$\frac{[R_{clr}(13.3) - R_{cld}'(13.3)]}{[R_{clr}(11.0) - R_{cld}'(11.0)]} < \frac{[R_{clr}(13.3) - R_{cld}(13.3)]}{[R_{clr}(11.0) - R_{cld}(11.0)]} , \quad (9)$$

or $L' < L$, where L refers to the left side of Eq. (3). An example plot of P_c versus R (where R refers to the right side of Eq. (3)), shown in Figure 2, indicates that $L' < L$ implies $P_c' > P_c$. Thus, when calculating a cloud pressure for the upper semi-transparent cloud layer in a two cloud layer situation, the CO_2 slicing algorithm places the upper cloud layer too low in the atmosphere.

An example from 25 October 1990 is presented to illustrate further the magnitude of the errors that can be induced by lower level clouds (results for other days and other situations were found to be comparable). Ground observers in Omaha, Nebraska reported thin cirrus clouds with no other underlying clouds present. The ratio of the 13.3 to 11.0 micron satellite observed radiance differences between clear and cloudy FOVs (the left side of Eq. (3)) is 0.37 on 25 October. This implies single layer cloud at 300 mb (solving the right side of Eq. (3) for P_c as shown in Figure 2).

As explained above, if there had been an opaque cloud layer below 300 mb, R_{cld}' would have been smaller than measured for these cases. The changes in R_{cld}' were modelled for underlying opaque cloud layers at 920, 780, 670, 500, 400 and 300 mb (producing different ratios L' in the left side of Eq. (3)). These changes will suggest different P_c' solutions as R, the right side of Eq. (3), is matched to L'. In the absence of any knowledge of a lower layer, the CO_2 algorithm incorrectly integrates from the surface to an incorrect P_c' (rather than from the lower cloud pressure to the correct upper cloud pressure). Figure 2 shows R as a function of P_c for the situation of 25 October. The errors in calculated cloud top pressure from the original 300 mb solution, P_c'-P_c, are shown as a function of height of the underlying opaque cloud layer in Figure 3 for 25 October.

In the two cloud layer situation, the position of the lower cloud layer affects the accuracy of the estimate of the height of the upper cloud layer. Opaque clouds in the lower troposphere near the surface underneath high cirrus have little affect on the cirrus P_c. While the 13.3 micron channel senses only about half of the radiation from below 800 mb, the infrared window channel sees mostly low in the atmosphere. Opaque clouds in the middle troposphere, between 400 and 800 mb, underneath high cirrus, cause the cirrus P_c to be substantially overestimated (lower in the atmosphere); largest errors occur for the very thin high cirrus cloud. The decreases in R_b produce smaller ratios for the left side of Eq. (3) which in turn produces larger estimates of P_c. Opaque clouds high in the atmosphere, underneath higher cirrus, have little effect on the cirrus P_c, since the height of the lower opaque layer approaches the height of the semi-transparent upper cloud layer and the CO_2 algorithm is going to estimate a height in between the two layers.

The errors in P_c were examined for different emissivities of transmissive clouds (see Figure 3). This was modelled by varying the emissivity and forming new ratios on the left side of Eq. (3). The maximum cloud top pressure error of roughly 290 mb occurred in very thin cloud with emissivity of .10. The error in P_c reduced as the emissivity of the transmissive clouds increased. For a cloud with emissivity of 0.5, the maximum error in P_c is about 80 mb. For more dense clouds with emissivity of 0.9, the maximum error in P_c is less than 20 mb. The GOES VAS data have shown a nearly uniform population of emissivity center around 0.5 (Wylie and Menzel, 1989), so one can conclude that the errors in the cloud top pressure caused by underlying clouds should average under 120 mb.

To minimize these errors, an algorithm is being developed to evaluate the cloud clusters in plots of CO_2 and IR window radiances within the target area, and then to use the radiances from these clusters to estimate the cloud top pressures of the lowest and highest cloud layers. The lowest cloud cluster belongs to the largest radiances that are not representative of the earth surface. A CO_2 slicing height is determined for this cluster. The highest cloud cluster belongs to the smallest radiances; a CO_2 height is determined for this cluster using the pressure of the lowest cloud cluster in the target area as the surface pressure in Eq. (3). Early attempts with this algorithm have been encouraging but further testing and refinement is still necessary; the two layer algorithm is not part of the improved NESDIS/CIMSS winds system yet.

5. Early Results

The improved winds algorithm has been running daily in a test mode at 1200 UT during September 1991. Global wind vectors are produced automatically with CO_2 slicing or IR histogram height assignments. The autoediter than adjusts and edits the vectors. No manual editing has been performed, although NESDIS intends to edit the data when operations begin. Comparisons with respect to radiosonde observations over North America are made if collocations are within 1 degrees latitude/longitude and within 90 minutes. The same is also done for the model first guess, which is the six hour aviation forecast from the National Meteorological Center. Sample statistics for the middle and high winds from 21 through 23 September are presented in Table 1.

The autoediting is improving the rms error in this small sample, most dramatically in the mid levels. The rms differences of the high level winds for both model and autoedited satellite are comparable, while for the middle level winds the autoedited satellite has smaller differences with respect to the radiosonde wind observations. In all cases rms vector differences are less than 7.0 m/s. This encouraging start is even more encouraging when it is remembered that the satellite winds have not been manually edited; it is reasonable to expect that manual editing will improve the satellite wind estimation performance.

Table 1. Sample statistics of vector differences (rms in meters/second) from 21-23 September 1991 of the NESDIS/CIMSS winds algorithm (without any manual editing) for high (above 350 mb) and middle (above 700 mb and below 350 mb) winds compared to the radiosonde winds. The same is also presented for the model first guess compared to radiosonde winds.

Level	Number	Model minus Raob rms	Sat Wind minus Raob rms
All	41	5.6	8.8 (unedited)
	30	6.1	5.9 (autoedited)
High	21	6.6	7.2 (unedited)
	20	6.6	6.9 (autoedited)
Mid	20	4.5	10.3 (unedited)
	10	4.8	3.0 (autoedited)

6. Future plans

NESDIS/CIMSS have been implementing and testing the improved winds algorithm for most of 1991. It is planned to begin operational utilization for full disk winds four times per day with the new software in December 1991. Low level winds will be produced by picture pair techniques and middle and high level winds from the CO_2 software.

Acknowledgements

The winds testing has involved Chris Velden, Tim Schmit, Kurt Brueske, Tony Schreiner, Barry Rowe, and Bob Merrill of CIMSS and Kit Hayden, Geary Callan, Cecil Paris, Curtis Holland, Glen Rutledge, Roney Sorenson, Jim Lynch, and Gene Legg of NESDIS. Dennis Deaven, Geoff DiMego, Paul Julian, Dennis Keyser, and Wayman Baker of NMC have assisted with the model impact tests. This work was supported by NOAA contract 50-WCNE-8-06058.

References

Eyre, J. R., and W. P. Menzel, 1989: Retrieval of cloud parameters from satellite sounder data: A simulation study. J. Appl. Meteor., 28, 267-275.

Green, R., G. Hughes, C. Novak, and R. Schreitz, 1975: The automatic extraction of wind estimates from VISSR data. NOAA Technical Memorandum NESS 64, 94-110.

McIDAS Applications Guide, 1988. Cloud Drift Winds. A Space Science and Engineering Center Manual.

Menzel, W. P., W. L. Smith, and T. R. Stewart, 1983: Improved cloud motion wind vector and altitude assignment using VAS. J. Clim. Appl. Meteor., 22, 377-384.

Menzel, W. P., D. P. Wylie, and K. I. Strabala, 1991: Seasonal and Diurnal Changes in Cirrus Clouds as seen in Four Years of Observations with the VAS. Jour. Appl. Meteor., in press.

Merrill, R., 1989. Advances in the automated production of wind estimates from geostationary satellite imaging. Fourth Conference on Satellite Meteorology, AMS, San Diego, CA, 16-19 May 1989

Merrill, R. T., W. P. Menzel, W. Baker, J. Lynch, E. Legg, 1991: A Report on the Recent Demonstration of NOAA's Upgraded Capability to Derive Satellite Cloud Motion Winds. Bull. Amer. Meteor. Soc., 72, 372-376.

Wylie, D. P., and W. P. Menzel, 1989: Two years of cloud cover statistics using VAS. J. Clim. Appl. Meteor., 2, 380-392.

Figure Captions

Figure 1. Flow chart of the CIMSS experimental wind system. Highlighted processes have been substantially upgraded in the past year. Boxes enclose processes, and dashed outlines define single job steps on the UW McIDAS.

Figure 2. The calculated ratio from the right side of Eq. (3) as a function of cloud top pressure for the sounding of 25 October 1990. The measured ratio from the left side of Eq. (3) is indicated. The cloud top pressure is inferred to be 300 mb.

Figure 3. The errors in calculated cloud top pressure (from the original 300 mb solution) for several different $N\epsilon$ as a function of height of the underlying opaque cloud layer.

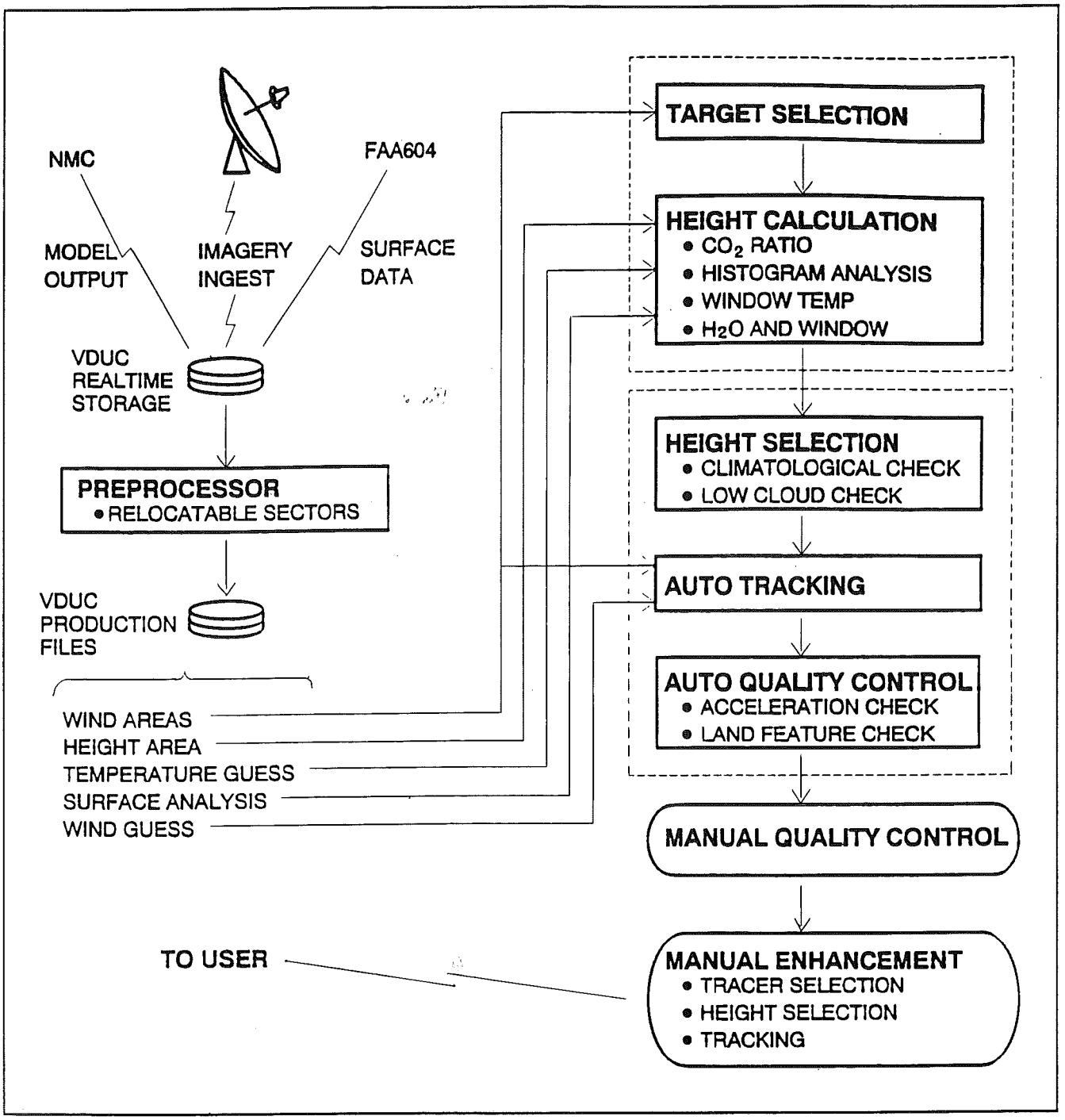

Figure 1. Flow chart of the CIMSS experimental wind system. Highlighted processes have been substantially upgraded in the past year. Boxes enclose processes, and dashed outlines define single job steps on the UW McIDAS.

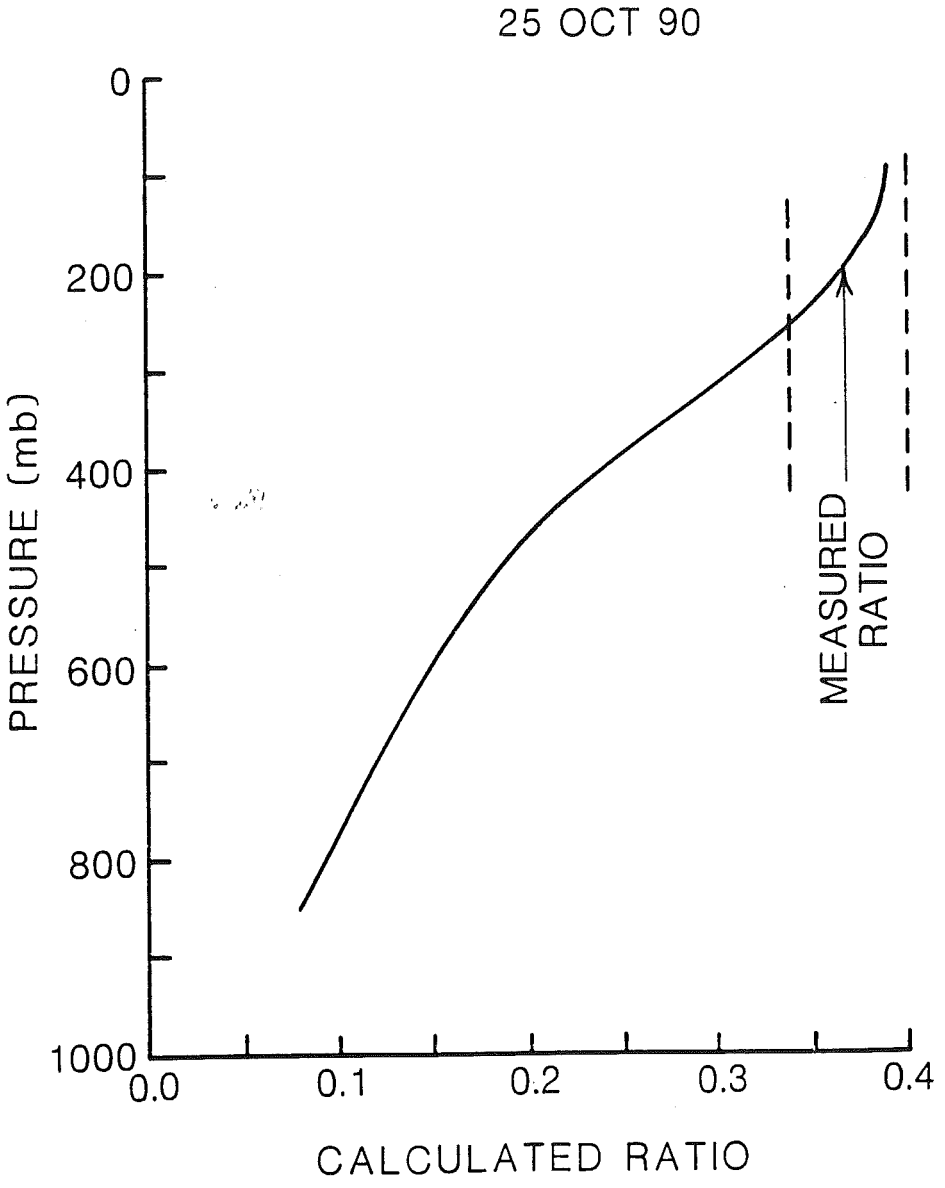

Figure 2. The calculated ratio from the right side of Eq. (3) as a function of cloud top pressure for the sounding of 25 October 1990. The measured ratio from the left side of Eq. (3) is indicated. The cloud top pressure is inferred to be 300 mb.

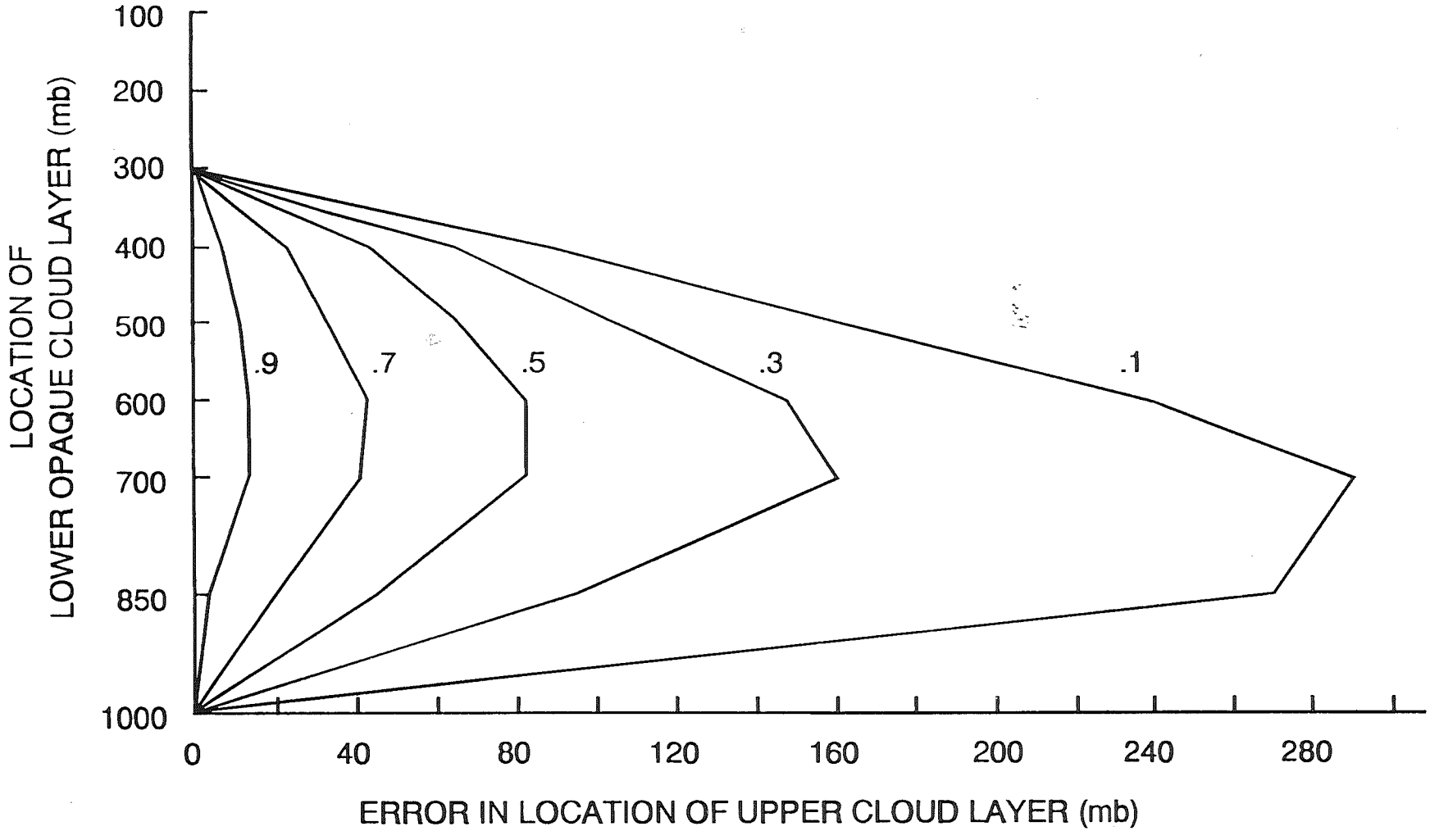

Figure 3. The errors in calculated cloud top pressure (from the original 300 mb solution) for several different $N\epsilon$ as a function of height of the underlying opaque cloud layer.